Numerical simulation of rotational flow in hydrocephalic hydro-elastic models

[1]Hemalatha Balasundaram, [2]Senthamilselvi Sathyamoorthi, [3]Ambrose Prabhu R, [4]Shyam Sundar Santra

[1,3]Rajalakshmi Institute of Technology, Chennai, Tamilnadu, India.

[2]Vels University, Pallavaram, Chennai, Tamilnadu, India.

[4]Department of Mathematics, JIS College of Engineering, Kalyani, West Bengal 741235, India

Abstract

Three-dimensional computational models of the cerebrospinal fluid (CSF) flow and brain tissue are presented for evaluation of their hydrodynamic conditions before and after shunting for seven patients with non-communicating hydrocephalus. We have developed a mathematical model of the fluid flow in cerebral ventricles during hydrocephalus is presented. The fluid-solid interaction simulation shows the CSF mean pressure is five times greater than normal subject. We present a brief overview of the clinical problems that are being addressed. This suggests that functional deficits observed in hydrocephalic patients could therefore be more related to the damage to periventricular white matter. we believe more accurately represent the anatomy of the brain and including time dependence.

Introduction

Many researchers have constructed computational models of hydrocephalus based on poroelasticity theory. Such models, it is thought, would provide greater comprehension of the problem and, as a result, better therapy. These existing poro elastic models only include hydrocephalus in its final sick form, not the transition from a healthy to a pathological state of the brain while the aqueduct is still open. Such models have also neglected to account for the intermittent effects of shunting, the most often utilized treatment for hydrocephalus. We use elasticity and fluid mechanics to create a mathematical model of the human brain and ventricular system. The model is used to research hydrocephalus, a pathological condition in which the normal flow of cerebrospinal fluid is disrupted, causing the brain to distort. Our model expands previous work in this area by considering flow across the aqueduct and including boundary constraints. This allows us to create a quantitative model of the start, improvement, and therapy of this disorder. We develop and solve the governing equations and boundary conditions for this model along with meaningful clinical findings.

CSF runs from production sites in the choroid plexuses of the lateral and third ventricles down a single thin cerebral aqueduct and into a fourth ventricle in a healthy brain. Our model expands earlier research on hydrocephalus by incorporating aqueduct flow with boundary constraints. A small quantity of fluid travels down the subarachnoid space around the spinal cord and then back up into the cranial subarachnoid space, however, the laws of physics make it difficult to explain how this flow could possibly be endured.

The dynamic interaction of pulsatile blood, brain, and CSF was studied using a mathematical framework that was based on in vivo inputs[1]. The simulation proposed in this paper is obtained

for CSF physio-pathological disease hydrocephalus patients[2]. An analysis of the lateral ventricular elasticity for congenital hydrocephalus in an asymmetric flow with species concentration[3].The present study while using a simple geometric model provides a new direction in multi-physical transport phenomena in the hydrocephalus and furthermore a benchmark for more geometrically complex simulations[4]. The equations of motion for CSF flow in the ventricular and subarachnoidal pathways as well as CSF seepage inside the porous brain parenchyma were solved. The boundary conditions for the complex brain geometry were formulated[5].

The experimental data was obtained from a normal subject and compared with a three-dimensional computational model of intracranial dynamics. Developed from subject-specific MR images, and using physiological boundary conditions as input, the model reproduces pulsatile CSF motion and predicts intracranial pressures and flow rates[6].The numerical model was employed to investigate the effects of cross-sectional geometry and spinal cord motion on unsteady velocity, shear stress, and pressure gradient fields[7]. The system was divided into five submodels representing arterial blood, venous blood, ventricular CSF, cranial subarachnoid space, and spinal subarachnoid space. These submodels are connected by resistance and compliance. The model developed was used to reproduce certain functional characteristics observed in seven healthy volunteers, such as the distribution (amplitude and phase shift) of arterial, venous, and CSF flows[8].

Time-resolved three-dimensional magnetic resonance velocity mapping has previously been used to investigate normal and pathologic blood flow patterns in the human vascular system. Here we used this technique to study the spatial and temporal dynamics of CSF flow in the ventricular system of 40 normal volunteers[9].

CSF is absorbed in the arachnoid villi, which are small granulations located inside the arachnoid that provide into the dura mater. The barrier among CSF and blood in these granulations is minimal, allowing CSF to flow into the circulation and be absorbed. In contrast to CSF production, consumption is pressure-dependent, with the rate influenced by the differential between intraventricular and superior sagittal venous pressure. In the present study, these effects and ICC diagrams have been investigated using 3D FSI simulation up to 2.5 years after shunt surgery in a large number of NCH patients through a non-invasive method[10].

A finite element parametric investigation on a head model under different scenarios of impact is conducted. In the study, the CSF material parameters are varied within the expected range of change, while other components of the head model are kept constant[11]. There is in the literature the descriptors, connecting and non-connecting hydrocephalus to distinguish cases where the aqueduct is open or blocked but since we are interested in the whole range of states of the aqueduct we shall not use these here. The most frequent cause of congenital and infantile hydrocephalus is a malformation in one or more parts of the ventricular system, for example, stenosis of the aqueduct or membranous occlusion of the foramen of Monro.

In this chapter, we build a model of the brain and ventricular system that is complicated enough to simulate the behavior of the hydrocephalic brain while residing simple sufficient for it to be mathematically accessible, and we use it to investigate the development and treatment of the disorder. The fluid dynamics of CSF circulation inside the skull system are oscillatory. The ventricular area equation of motion inside the porous medium with adequate pulsatile boundary conditions was simulated. The simulation proposed in this article is

obtained for patients with CSF physiopathological illness hydrocephalus. Using appropriate validity, we calculated the CSF flow velocity of patients.

Mathematical Formulation

The CSF is regarded as a Newtonian fluid in this investigation, with dynamic viscosity and density of 1.003 x 10(-3) kg/ms and 998.2 kg/m3, respectively [1]. The brain tissue is classified as a linearly viscoelastic material, with storage and loss moduli of 2038 and 1356 Pa for healthy subjects, respectively, and 1594 and 1015 Pa for patients, and a density of 1040 kg/m3 [8, 9]. The lateral ventricles have a CSF flow rate of 0.35 cm3/min [1]. For numerical models, this number is employed as the value of the amplitude in the input fluids pulsatile flow rate function—the final segment of the ventricular system following the fourth ventricle is chosen as the flow output site. The usual baseline CSF pressure was established at 500 Pa, whereas the pathological baseline was set at 2700 Pa [6].

$$\frac{\partial u_c}{\partial x} + \frac{\partial w_c}{\partial y} = 0$$

$$\frac{\partial u_c}{\partial t} + Gw_0 \frac{\partial u_c}{\partial y} + 2\Omega' w_c = -\frac{1}{\rho}\frac{\partial p}{\partial x} + \nu\left(\frac{\partial^2 u_c}{\partial y^2}\right) - \frac{RN}{\rho} u_c$$

$$\frac{\partial u_c}{\partial t} + Gw_0 \frac{\partial w_c}{\partial y} - 2\Omega' u_c = -\frac{1}{\rho}\frac{\partial p}{\partial x} + \nu\left(\frac{\partial^2 w_c}{\partial y^2}\right) - \frac{RN}{\rho} w_c$$

$$u_c = \omega\left(\mathrm{Cos}\,\omega t + \tfrac{1}{2} Sin\omega t\right), w = 0, \text{ at } y = 0 \; and \; t \leq 0$$

$$u = u_0\omega, w = 0 \text{ at } y = 1\,, t > 0$$

Let's consider the pressure difference exponentially transverse concerning angular velocity $\frac{\partial p}{\partial x} = \omega e^{-\omega t}$. We used pulsatile inlet boundary condition [14] to approach the CSF flow in the parenchymal layer. The dimensionless quantities for the problem by neglecting the dash for our convenience

$$y' = \frac{y}{l},\; t' = \frac{tw_0}{l},\; w' = \frac{wl}{w_0},\; u_c{}' = \frac{u_c}{u_0},\; \omega' = \frac{\omega l^2}{\nu}$$

$$\theta' = \frac{T - T_c}{T_0 - T_c},\; Re = \frac{w_0 l}{\nu}, G_{pm} = \frac{RNl^2}{\mu}, \Omega' = \frac{\Omega l^2}{\nu}$$

u and w represent the CSF velocity of the fluid in x & y direction respectively. w_0 represents characteristic velocity. Fluid density is denoted as ρ. Da and Ω are expressed as darcy number and angular velocity, G_{pm} referred as particle mass parameter. ω denotes CSF Womersley number.

The above governing equations dimensionalised and hence the dimensionless form of the same with suitable boundary conditions is represented as follows

$$Re\left(\frac{\partial u_c}{\partial t}+G\frac{\partial u_c}{\partial y}\right)+2\Omega w=-\alpha^2e^{\varphi t}+\frac{\partial^2 u_c}{\partial y^2}-G_{pm}u_c \quad (1)$$

$$Re\left(\frac{\partial w_c}{\partial t}+G\frac{\partial w_c}{\partial y}\right)-2\Omega W_c=-\alpha^2e^{\varphi t}+\frac{\partial^2 w_c}{\partial y^2}-G_{pm}W_c \quad (2)$$

$u_c=\alpha^2\left(\text{Cos}\,\varphi t+\frac{1}{2}Sin\varphi t\right), W_c=0\ at\ y=0$

$u_c=\alpha^2\,\text{Cos}\,n\varphi t\,, w=0\ at\ y=1$. Were n being an integer.

u and w are functions of x and y, as we considered the fluid flows rotationally. To solve the above momentum equation the complex function $F_c=u+iw$ is used, Navier Stoke's equation in an explicit form of complex function with boundary conditions is followed as

$$Re\left(\frac{\partial F_c}{\partial t}+G\frac{\partial F_c}{\partial y}\right)+2\Omega IF_c=-2I\alpha^2e^{\varphi t}+\frac{\partial^2 F_c}{\partial y^2}-G_{pm}F_c \quad (3)$$

$F_c=\alpha^2\left(\text{Cos}\,\varphi t+\frac{1}{2}Sin\varphi t\right), y=0, t\le 0$

$F_c=\alpha^2\,\text{Cos}\,n\varphi t\,, y=1, t>1$

METHOD OF SOLUTION

We use analytical tools and a model issue to understand the biologically beneficial nature of the brain's systems and their physical consequences. The statistical approach may improve the efficacy of the numerical method. Consequently, we simplify those equations into ordinary differential equations and solve them analytically. We solve the governing equation utilizing the perturbation approach as it is error-free, adopting the trial solution for velocity.

$$F_c(y,t)=F_0(y)+\frac{\epsilon}{2}e^{i\lambda t}F_1(y)+\frac{\epsilon}{2}e^{-i\lambda t}F_2(y) \quad (4)$$

λ denotes oscillation frequency and ϵ an arbitrary constant parameter with $\epsilon \ll 1$. Consider u_0, u_1, u_2 refers base part, perturbed part first order and perturbed part second orders of conservation of momentum respectively. F and u's complex parameters are encoded by I, i.

The analytical perturbation strategy is used to solve the given problem, yielding

$$F_0=\alpha^2e^{\,m_1y}-A_2(e^{\,m_1y}-e^{\,m_2y})+\frac{2\alpha^2}{a}(e^{\,m_1y}-1) \quad (5)$$

$$F_1=\alpha^2\left(\cos\varphi t+\tfrac{1}{2}sin\varphi t\right)e^{\,m_3y}-\frac{(e^{\,m_3y}-e^{\,m_4y})}{(e^{\,m_3}-e^{\,m_4})}\left[\alpha^2\left(\cos\varphi t+\tfrac{1}{2}sin\varphi t\right)e^{\,m_3}-\right.$$

$$\left.\alpha^2\cos\varphi t+\frac{2\alpha^2e^{\varphi t}}{b}(e^{\,m_3}-1)\right]+\frac{2\alpha^2}{a}(e^{\,m_1y}-1) \quad (6)$$

$$F_2 = \alpha^2\left(\cos\varphi t + \frac{1}{2}sin\varphi t\right)e^{m_5 y} - \frac{(e^{m_5 y} - e^{m_6 y})}{(e^{m_5} - e^{m_6})}\left[\alpha^2\left(\cos\varphi t + \frac{1}{2}sin\varphi t\right)e^{m_3} - \alpha^2\cos\varphi t + \frac{2\alpha^2 e^{\varphi t}}{b}(e^{m_5} - 1)\right] + \frac{2\alpha^2}{a}(e^{m_1 y} - 1) \quad (7)$$

RESULT AND DISCUSSION

To investigate the different physical characteristics such as dynamic viscosity, density, kinematic viscosity, resistance parameter, Elastic parameter, Reynolds number, and Womersley number were calculated analytically and the results are shown below. The intracranial pressure of normal subject human beings was found to be 500Pa and 3000Pa for hydrocephalus patients [14]. The size of the lateral ventricle in hydrocephalus is much larger than normal when CSF flows. As a result, there is a significant statistical difference in the expansion of the ventricular for hydrocephalus. To employ the behaviour of CSF for hydrocephalic patients we use the following parameters Porosity (0.25), Pressure gradient (2700), Elasticity(350Pa), Reynolds Number (468.3), Womersley Number (more than 8.9) and Resistance parameter (1.367).The graphs shows Velocity profile(cm/s) in y axis and Time ‘t’ along x axis.

Fig 1 exploits the variation of the Reynolds number with time variation. Re varies from 130, 240,420 has been depicted for CSF with hydrocephalus subjects. Here it is shown that the velocity increases as the when Reynolds number escalates with time taken for cardiac cycle.

When the flow fluctuates during the early systole of the cardiac cycle, the velocity of CSF flow reaches a peak. When the frequency increases over time, the circulation rate of hydrocephalus reduces. As a result, increasing the Womersley number for pulsatile flow to 6.2, 7.5, or 8.9 with variable velocity yields the optimum volumetric flow rate. Fig: 4.

The greatest amount of hydrocephalus is reached in Fig 2 with varied Resistance parameters 0.9, 1, 1.36. Furthermore, when the fluid level increases, the ventricular flexibility deforms (see Fig 3). The brain parenchyma porosity is estimated to be 0.2 [4]. As a result, the fluid velocity increases as the permeability increases, demonstrating the elevated pressure of the CSF fluid flow.The pressure of hydrocephalus is close to 3000Pa whereas for normal subjects

is ≤500Pa [1]. We validate the increase in pressure graphically in Fig:5.

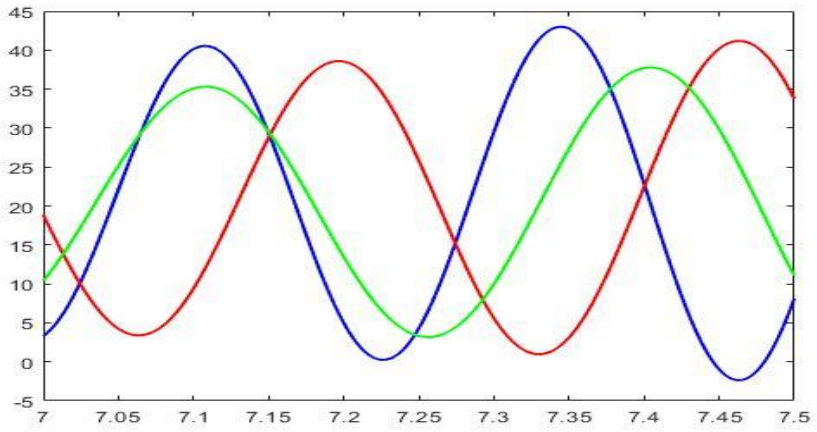

Fig: 1 Velocity profile with varying Reynolds number

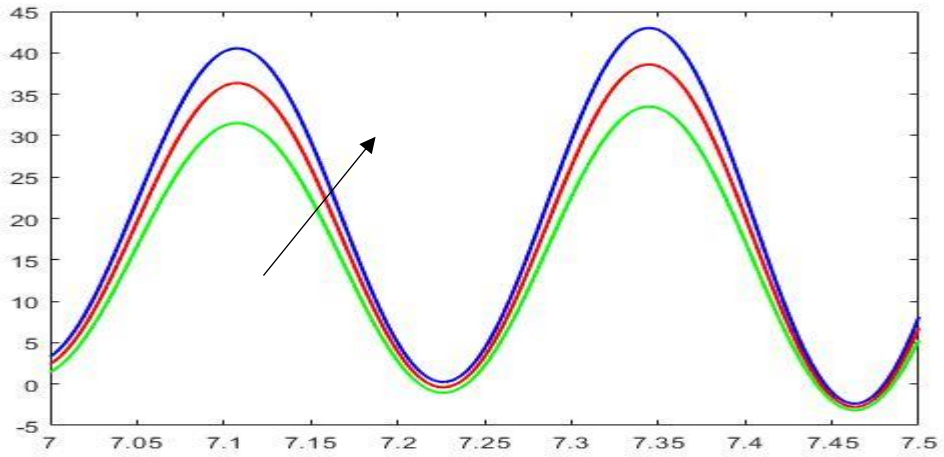

Fig: 2 Velocity profile with varying particle mass parameter

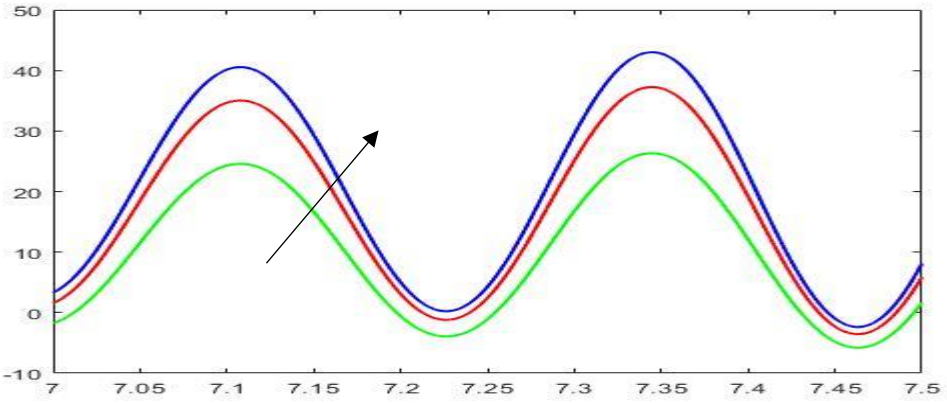

Fig: 3 Velocity profile with varying Elasticity

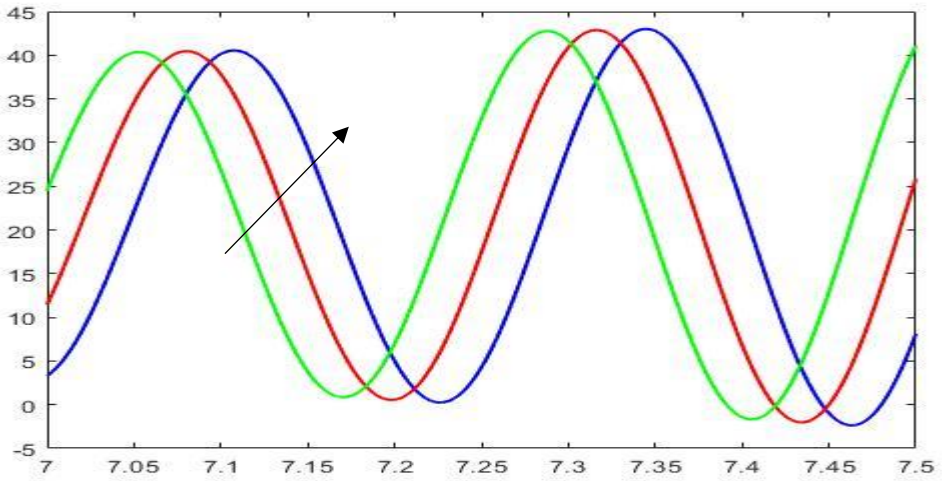

Fig: 4 Velocity profile with varying Womersley number

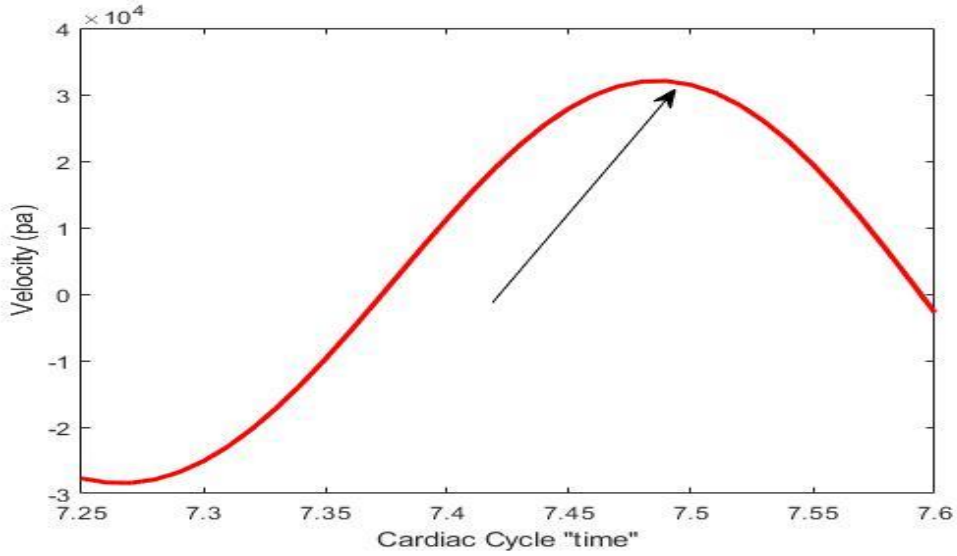

Fig: 5 Pressure of CSF from Velocity profile with varying with time ‘t’

CONCLUSION

In response to the impacts of high CSF pulsatile velocity, the hydrocephalus pressure differential in the brain fluctuates greatly. This leads to increased cranial system ventricular hypertrophy, as seen by the elasticity graph. When there is a rise in pressure, there is less ventricular compliance. CSF circulation as well as production will have an impact on the complete function of afflicted patients, resulting in brain damage.

The flow level in the cardiac cycle is predicted by important characteristics such as Womersley number, elasticity, particle mass parameter, and Darcy number. This work verified a few noteworthy properties of fluid behavior in thermal transfer in a simplified representation of hydrocephalus useful for neurological studies. The following are the findings from the current study.

The momentum of fluid flow increases as the Darcy number, resistance parameter, Womersley number, and Reynolds number increase. Increased deformation (elasticity) caused by dimensional change increases cerebrospinal fluid velocity.

References

1. Gholampour, Seifollah, et al. "A mathematical framework for the dynamic interaction of pulsatile blood, brain, and cerebrospinal fluid." *Computer Methods and Programs in Biomedicine* 231 (2023): 107209.
2. Balasundaram, Hemalatha, et al. "Hydrocephalic cerebrospinal fluid flowing rotationally with pulsatile boundaries: A mathematical simulation of the thermodynamical approach." *Theoretical and Applied Mechanics Letters* 13.1 (2023): 100418.
3. Balasundaram, H., et al. "Effect of Ventricular Elasticity Due to Congenital Hydrocephalus. Symmetry 2021, 13, 2087." (2021).
4. Gholampour, S., et al. "Numerical simulation of cerebrospinal fluid hydrodynamics in the healing process of hydrocephalus patients." *Journal of Applied Mechanics and Technical Physics* 58 (2017): 386-391.
5. Linninger, Andreas A., et al. "Cerebrospinal fluid flow in the normal and hydrocephalic human brain." *IEEE Transactions on Biomedical Engineering* 54.2 (2007): 291-302.
6. Sweetman, Brian, et al. "Three-dimensional computational prediction of cerebrospinal fluid flow in the human brain." *Computers in biology and medicine* 41.2 (2011): 67-75.
7. Loth, Francis, M. Atif Yardimci, and Noam Alperin. "Hydrodynamic modeling of cerebrospinal fluid motion within the spinal cavity." *J. Biomech. Eng.* 123.1 (2001): 71-79.
8. Ambarki, Khalid, et al. "A new lumped-parameter model of cerebrospinal hydrodynamics during the cardiac cycle in healthy volunteers." *IEEE transactions on biomedical engineering* 54.3 (2007): 483-491.
9. Stadlbauer, Andreas, et al. "Insight into the patterns of cerebrospinal fluid flow in the human ventricular system using MR velocity mapping." *Neuroimage* 51.1 (2010): 42-52.
10. Gholampour, Seifollah. "FSI simulation of CSF hydrodynamic changes in a large population of non-communicating hydrocephalus patients during treatment process with regard to their clinical symptoms." *PloS one* 13.4 (2018): e0196216.
11. Chafi, M. Sotudeh, et al. "A finite element method parametric study of the dynamic response of the human brain with different cerebrospinal fluid constitutive

properties." *Proceedings of the Institution of Mechanical Engineers, Part H: Journal of Engineering in Medicine* 223.8 (2009): 1003-1019.